RSC Advances

ROYAL SOCIETY OF CHEMISTRY

www.rsc.org/advances

Synthesis of Ni_3N/SiO_2 Nanocomposites and Investigation of Their Intrinsic Static and Dynamic Magnetic Properties

Yongshuai Jia[a], Haoshuai Pan[a], Hongjie Meng[a, b], Haojie Liu[a, b], Zeqian Wang[b], Xiao Li[b], Longlong Zhu[b], Peng Chai[b], Chunhong Gong[a, b*]

[a]*Key Laboratory for Special Functional Materials of the Ministry of Education, Henan University, Kaifeng 475004, China;*

[b]*College of Chemistry and Chemical Engineering, Henan University, Kaifeng 475004, China*

*Corresponding author

College of Chemistry and Chemical Engineering, Henan University, Kaifeng 475004, China

E-mail address: gongch0378@foxmail.com, TEL.: +86 -378-23881358

Ni_3N/SiO_2 nanocomposites were prepared *via* nitriding of Ni/SiO_2 nanocomposite precursor in flowing ammonia. The intrinsic static and dynamic magnetic properties of as-prepared samples were investigated with a superconducting quantum interference device and an Agilent N5230A network analyzer, respectively. According to our results, it was found that pure phase nanocrystalline Ni_3N could be obtained after Ni/SiO_2 nanocomposite precursor was calcined under a flow of NH_3 at 300 ^oC, and as-obtained nanocrystalline Ni_3N is non-ferromagnetic under the static magnetic field and non-magnetic under the dynamic electromagnetic field.

1. Introduction

The 3d transition metal nitrides are an interesting set of compounds that possess unique phase relationships, crystal structures, and optical, electronic and magnetic properties. Detailed information about the relative stability, structures, as well as the electronic and magnetic properties of the phases is of great interest for scientists in the fields of physics, chemistry and materials science.[1,2] For example, some nitrides of transition metals and alloys can be used in corrosion resistant and optical coatings, electrical contacts, diffusion barriers, and magnetic data storage devices, while their corrosion resistance and magnetic properties such as magnetic moment and coercivity can be effectively manipulated by proper incorporation of nitrogen into the lattice.[3]

However, relevant researches mainly focus on transition metal nitrides with high melting point, and few are currently available about the synthesis and characterization of metastable metal nitrides (e.g., nitrides of Ni, Co, and Cu),[4] because metastable metal nitrides usually exhibit limited thermal stability and have complex phase diagrams that complicate the analysis of the experimental results.[5,6]

As a typical class of metastable nitride, Ni_3N has been known to be rather stable at room temperature and is a potential material in some applications in the recent literatures, [7] e.g., in lithium ion batteries[8,9] and in the field of catalysis.[10,11] Some primary researches demonstrate that Ni_3N can be obtained by heating a properly selected precursor, e.g., nickel metal, under ammonia flow.[12] In general, it is difficult to obtain pure samples with high homogeneity using those methods and the product is not pure-phase Ni_3N but actually a mixture of different nitride phases with very different physical properties or contain residual Ni metal, which adds to the diversity of the reported physical properties of as-synthesized Ni_3N.[13-16] Therefore, much remains to be clarified. For example, the magnetic properties of Ni_3N is still debated in the literature, Vempaire *et al* reported that Ni_3N phase is non-ferromagnetic,[14] but Gajbhiye *et al* claimed that Ni_3N phase is a ferromagnetic with a weak

saturation magnetization.[13] Such a diversification implies that it is imperative to develop a facile method for synthesizing highly pure Ni_3N so as to provide the prerequisite for accurately evaluating the magnetic state.

In the present research we adopt Ni/SiO_2 nanocomposite as a precursor to synthesize Ni_3N/SiO_2 composite *via* calcining in flowing ammonia. This strategy, thanks to the use of Ni powder with a samll size and the incorporation of SiO_2 matrix, helps to provide highly pure Ni_3N nanoparticles at a moderate nitriding temperature. This paper reports the synthesis of Ni_3N/SiO_2 nanocomposites at a relatively low temperature as well as gives unambiguous evidence for the their intrinsic static and dynamic magnetic properties.

2. Experimental

All the reagents are of analytical grade (Tianjin Kermel Chemical Company Ltd., Tianjin, China) and were used as-received. Based on our previous work, [17] Ni/SiO_2 nanocomposites were prepared and used as the precursors (denoted as S-0). In a typical process, 9.48 g of $NiCl_2 \cdot 6H_2O$, 40 mL of $N_2H_4 \cdot H_2O$ (80wt%), 1 g of NaOH, 200 mL of ethylene glycol, and 0.6 mL tetraethyl orthosilicate (TEOS) were uniformly mixed and the resultant mixture was heated to 70 ^oC and held there for 2-4 h. The resultant products were fully washed with ethanol, followed by drying in vacuum to afford Ni/SiO_2.Then, as-obtained Ni/SiO_2 was calcined in flowing ammonia at moderate temperatures of 280 ^oC, 300 ^oC, and 350 ^oC for 5-48 h yielding nitrided products denoted as S-280-5, S-300-5, S-300-12, S-300-24, S-300-48, and S-350-5, respectively.

The morphology of as-prepared samples was examined with a scanning electron microscope (SEM, JEOL JSM-5600LV) and a transmission electron microscope (TEM, JEOL JEM-2010). A Philips

X'Pert Pro X-ray diffractometer (XRD, Cu-*K*α radiation, λ = 1.5406 Å) was performed to analyze their phase compositions and microstructures. Magnetic measurements were conducted with a superconducting quantum interference device (SQUID, MPMS XL-7, Quantum Design). Moreover, for the measurements of dynamic magnetic properties, as-synthesized Ni_3N/SiO_2 nanocomposites were mechanically mixed with paraffin wax at a mass ratio of 1:1 and pressed into cylindrically shaped compacts; and then the complex permeability of the cylindrical compacts was recorded in the frequency range of 2.0~18.0 GHz with an Agilent N5230A network analyzer. Just like SiO_2, paraffin is a typical nonmagnetic and electromagnetic transparent material, which does not influence the native magentic and electrmagentic behavior of Ni_3N.[18, 19]

3. Results and discussion

The XRD patterns of as-synthesized precursor S-0 and various nitridation products are presented in Fig. 1. Precursor S-0 shows three characteristic peaks of face-centered cubic Ni (JCPDS 04-0850) at 2θ = 44.5º, 51.8º, and 76.4º. Differing from the precursor, sample S-280-5 shows a new XRD peak of Ni_3N aside from the XRD signal of Ni phase[5], which proves that 5 h-calcination of precursor S-0 in flowing ammonia at 280 ^oC produces Ni_3N *via* the reaction between Ni and NH_3:

$$3Ni + NH_3 = Ni_3N + 3/2H_2 \uparrow \quad (1)$$

As the calcination temperature is increased to 300 ^oC, resultant product, S-300-5, shows characteristic peaks of Ni_3N phase, and the diffraction peaks of Ni disappear. This suggests that pure-phase Ni_3N can be successfully synthesized through nitriding nanocrystalline nickel at 300 ^oC under atmospheric pressure. However, the diffraction peaks of S-300-5 are slightly deviated to higher 2θ as compared with the standard XRD peaks of Ni_3N (JCPDS 10-0280), which implies that the transformation from Ni

metal to Ni_3N, upon 5-h calcination in flowing ammonia at 300 °C, might be incomplete. When the calcination time is extended to 12 h under 300 °C, the diffraction peaks of resultant products, sample S-300-12, S-300-24 and S-300-48, match the standard XRD card of Ni_3N exactly, which means that the structure transition of the precursor is more completed thereat and this technique appears to be efficient for the synthesis of Ni_3N.

Interesting, sample S-350-5 shows only XRD signal of face-centered cubic Ni phase, which is because Ni_3N is a thermal unstable material and is decomposed to metallic nickel and nitrogen gas upon heating above its decomposition temperature:

$$2Ni_3N = 6Ni + N_2\uparrow \quad (2)$$

Therefore, it is suggested to calcine precursor S-0 at 300 °C for over 12 h in flowing NH_3 so as to harvest single-phase Ni_3N. Moreover, all as-synthesized products show no evident XRD peaks of SiO_2, which implies that SiO_2 in all as-synthesized Ni_3N/SiO_2 nanocomposites is of amorphous state.

As shown in Fig. 2, as-prepared Ni/SiO_2 and Ni_3N/SiO_2 nanocomposites appear similar morphology as irregular spheres and have an average size of 200 nm, which indicates that 300 °C calcination play very little affect on the morphology and size of the obtained particles.

The room temperature magnetic hysteresis (denoted as *H)* loops of various Ni_3N/SiO_2 nanocomposites obtained under different nitriding conditions are shown in Fig. 3. It is seen that precursor S-0 has a high saturation magnetization and a low coercivity, which means that the precursor is softly ferromagnetic. As the precursor is heated at 280 °C for 5 h in flowing ammonia, resultant product, S-280-5, exhibits a lower saturation magnetization of 19.1 $emu \cdot g^{-1}$ than the precursor (26.1 $emu \cdot g^{-1}$). In combination with relevant XRD results, it can be supposed that the weak ferromagnetic signal of S-280-5 could be assigned to residual non-nitrided nickel in association with inadequate degree of nitriding at moderate

calcination temperature. As the calcining temperature is increased to 300 °C, for sample S-300-5, most of the starting ferromagnetic nickel has been transformed into non-ferromagnetic nickel nitride and a decrease of 99.8% of the magnetization is observed, which was assigned to residual non-nitrided nickel and is in agreement with results of some present studies (Fig. 3(a)) [7]. Furthermore, the M (H) typical loops of Ni_3N obtained at a longer time are still provided as a comparison (Fig. 3(b)). As expected, it was found that the magnetization of as-prepared Ni_3N nanoparticles decreased sharply with extending nitridation time, which could be due to the adequate degree of nitriding. More importantly, when the nitridation time is long enough (48h), there is no ferromagnetic signal could be detected in sample S-300-48, and the magnetic cycle could not saturate even added for a larger range of magnetic fields (±50 kOe) (Fig. 3(c) and (d)). With no ambiguity, it could be concluded that Ni_3N is a non-ferromagnetic material and the weak paramagnetic signals detected might attribute to residual paramagnetic impurities, which is consistent to the results of all theoretical studies.[20, 21]

Interestingly, when the nitriding temperature is elevated to 350 °C, resultant product, sample S-350-5, becomes typical soft ferromagnetic and exhibits a high saturation magnetization of 29.6 $emu \cdot g^{-1}$, which well conforms to the transformation from ferromagnetic Ni in the precursor to non-ferromagnetic Ni_3N and then to ferromagnetic Ni again, depending on varying calcining temperature. In general, the magnetic properties of nanosized and ultrafine magnetic materials are dependent on many factors, such as morphology, grain size, crystallinity and so on.[22] In the present research, the metallic nickel obtained form the decomposition of Ni_3N has a higher saturation magnetization than precursor S-0, which might be because the former has a cleaner surface and contains a decreased amount of surface defects.

Fig. 4 shows the frequency dependence of the complex relative permeability ($\mu_r = \mu_r' + i\mu_r''$) of precursor S-0 and products S-280-5, S-300-12, and S-300-48, where the real part of permeability (μ_r')

represents the magnetic energy storage and the imaginary part (μ_r''), refers to the energy loss. As shown in Fig. 4, along with the increase of nitriding degree, the real part of the complex permeability of Ni_3N/SiO_2 nanocomposites tends to approach to 1 in the whole test frequency, and the imaginary part of the complex permeability tends to approach to 0 therewith. Namely, the real part and imaginary part of the permeability of S-300-12 and S-300-48 obtained after complete nitriding are close to 1 and 0, respectively. This proves that pure phase Ni_3N has indeed no response to dynamic magnetic field, which is consistent with its non-ferromagnetic properties.

4. Conclusions

In summary, a facile route has been established to synthesize Ni_3N at a moderate temperature. The results indicate that calcining Ni/SiO_2 nanocomposite in flowing ammonia at properly selected temperature and duration facilitates the doping of N atoms into the Ni lattice thereby affording pure-phase Ni_3N *via* complete transformation from metallic Ni to the nickel nitride. The optimal calcination temperature and time are suggested as 300 ^oC and 48 h, under which Ni_3N exhibit a non-ferromagnetic nature under both static and dynamic electromagnetic fields is harvested. As the nitriding temperature is elevated to 350 ^oC, incorporated N atoms will escape from the Ni_3N lattice again thereby producing pure phase Ni whose saturation magnetization is even higher than that of the precursor S-0.

Acknowledgements

This research is supported by the National Natural Science Foundation of China (grant Nos. 50902045/E0213, 20971037/B0111, and 21271063).

References

1 C. Fang, R. Koster, W. Li, and M. Huis, *RSC Adv*, 2014, **4**, 7885.

2 E. Gregoryanz, C. Sanloup, M. Somayazulu, J. Badro, G. Fiquet, H. Mao, and R. Hemley, *Nat. Mater.*, 2004, **3**, 294.

3 R. Dubey, and A. Gupta, *J. Appl. Phys.*, 2005, **98**, 083903.

4 A. Baiker, and M. Maciejewski, *J. Chem. Soc.,* 1984, **80**, 2331.

5 Z. Wang, W. Yu, J. Chen, M. Zhang, W. Li, and K. Tao, *J. Alloy. Compd.,* 2008, **466**, 352.

6 P. Xi, Z. Xu, D. Gao, F. Chen, D. Xue, C.Tao, and Z. Chen, *RSC Adv*, 2014, **4**, 14206.

7 D. Vempaire, S. Miraglia, J. Pelletier, D. Fruchart, E.K. Hlil, L. Ortega, A. Sulpice, and F.Fettar, *J. Alloy. Compd.,* 2009, **480**, 225.

8 F. Gillot, J. Oró-Solé, and M. Palacín, *J. Mater. Chem.*, 2011, **21**, 9997.

9 X. Li, M. H. Mahboba, L. H. Andrew, and R. O. John, *J. Mater. Chem. A*, 2013, **1**, 6441.

10 G. Clavel, V. Molinari, A. Kraupner, and C. Giordano, *Chem. Eur. J.*, 2014, **20**, 9018.

11.M. Shalom , V. Molinari, D. Esposito, G. Clavel, D. Ressnig, C. Giordano, and M. Antonietti, *Adv. Mater.* 2014, **26,** 1272.

12 C. Guillaume, J. Morniroli, D. Frost, and G. Serghiou, *J. Phys - Condens. Mat.,* 2006, **18**, 8651.

13 N. Gajbhiye, R. Ningthoujam, and J. Weissmüller, *Phys. Status Solidi*, 2002, **189**, 691.

14 D. Vempaire, F. Fettar, L. Ortega, F. Pierre, S. Miraglia, A Sulpice, J. Pelletier, E.K. Hlil, and D.Fruchart, *J. Appl. Phys.,* 2009, **106**, 073911.

15 A. Linnik, A. Prudnikov, R. Shalaev, V. Varyukhin, S. Kostyrya, and V. Burkhovetskii, *Tech. Phys. Lett.*, 2012, **38**, 499.

16 A. Linnik, A. Prudnikov, R. Shalaev, T. Linnik, V. Varyukhin, S. Kostyrya, and V. Burkhovetskii,

Tech. Phys. Lett., 2013, **39**, 143.

17 C. Gong, X. Wang, X. Zang, X. Zhao, H. Meng, Y. Jia, W. Zhang, and J. Zhang, *Mater. Lett.*, 2014, **121**, 81

18 M. Cao, X. Shi, X. Fang, H. Jin, Z. Hou, W. Zhou, and Y. Chen, *Appl. Phys. Lett.*, 2007, **91**, 203110.

19 R. Zhuo, L. Qiao, H. Feng, J. Chen, D. Yan, Z. Wu, and P. Yan, *J. Appl. Phys.,* 2008, **104**, 094101.

20 C. Fang, M. Sluiter, M.van Huis, and H. Zandbergen, *Phys. Rev. B*, 2012, **86**, 134114.

21 D. Vempaire, J. Pelletier, A. Lacoste, S. Béchu, J. Sirou, S. Miraglia, and D. Fruchart, *Plasma Phys. Control. Fusion.,* 2005, **47**, A153.

22 C. Gong, J. Zhang, X. Zhang, L. Yu, P. Zhang, Z. Wu, and Z. Zhang, *J. Phys. Chem. C*, 2010, **114**, 10101.

Captions

Fig. 1. XRD patterns of as-prepared Ni/SiO_2 and Ni_3N/SiO_2 nanocomposites.

Fig. 2. SEM images of as-synthesized samples S-0 (a), S-300-12 (b), S-300-24 (c), and S-300-48 (d). The upper right inset shows the corresponding TEM image of S-300-24.

Fig. 3. Room temperature magnetic hysteresis loops of precursor S-0 and products obtained under different nitridation conditions.

Fig. 4. Frequency dependence of the complex relative permeability of precursor S-0 and products S-280-5, S-300-12, and S-300-48.

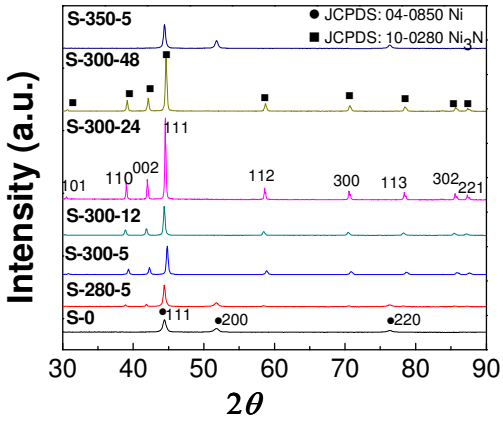

Fig. 1. XRD patterns of as-prepared Ni/SiO_2 and Ni_3N/SiO_2 nanocomposites.

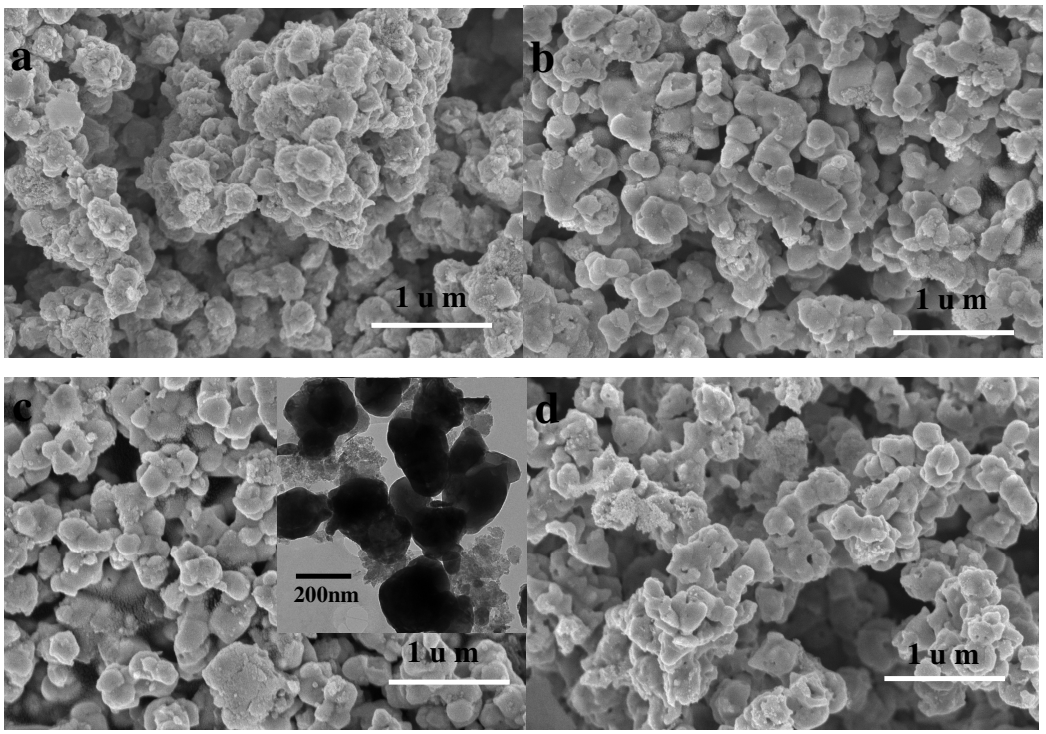

Fig. 2. SEM images of as-synthesized samples S-0 (a), S-300-12 (b), S-300-24 (c), and S-300-48 (d).

The upper right inset shows the corresponding TEM image of S-300-24.

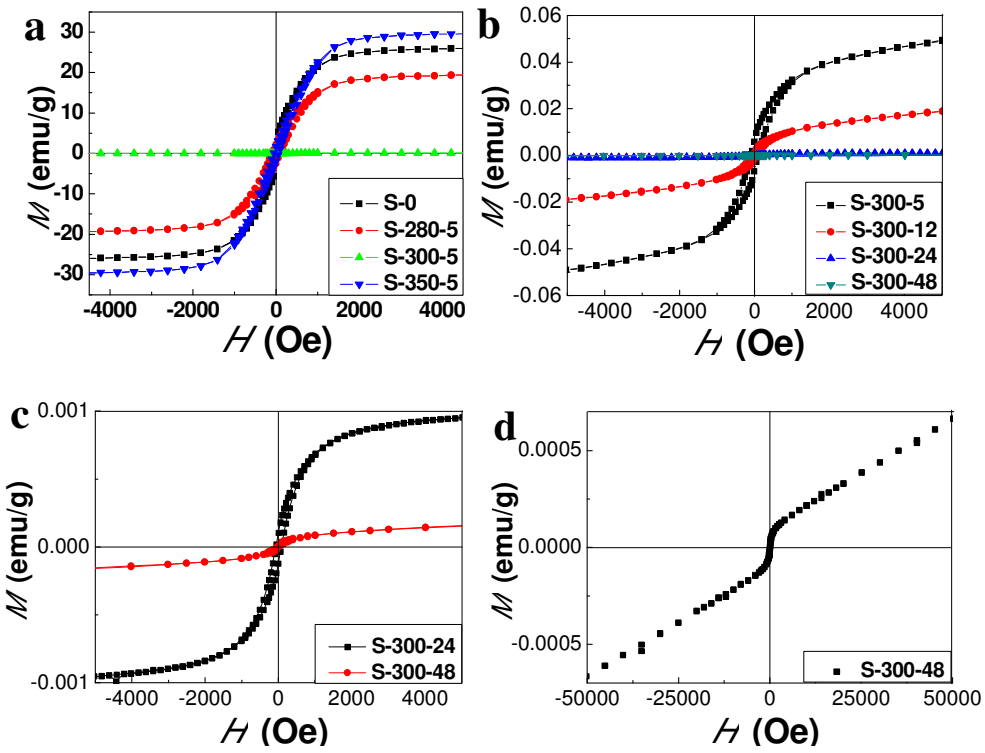

Fig. 3. Room temperature magnetic hysteresis loops of precursor S-0 and products obtained under different nitridation conditions.

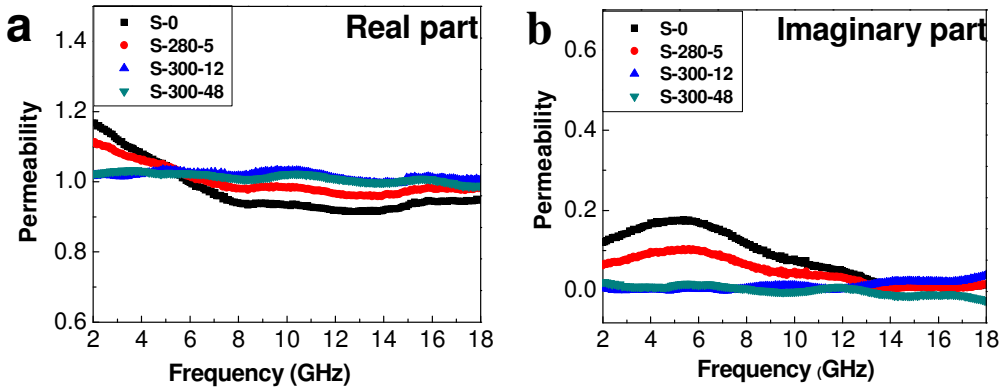

Fig. 4. Frequency dependence of the complex relative permeability of precursor S-0 and products S-280-5, S-300-12, and S-300-48.